

## Spin-orbit effects on resonant tunneling conductance through a double-quantum-dot system

This article has been downloaded from IOPscience. Please scroll down to see the full text article.

2008 J. Phys.: Condens. Matter 20 135221

(<http://iopscience.iop.org/0953-8984/20/13/135221>)

View [the table of contents for this issue](#), or go to the [journal homepage](#) for more

Download details:

IP Address: 129.252.86.83

The article was downloaded on 29/05/2010 at 11:16

Please note that [terms and conditions apply](#).

# Spin-orbit effects on resonant tunneling conductance through a double-quantum-dot system

Hong-Yi Chen<sup>1</sup>, Vadim Apalkov<sup>2</sup> and Tapash Chakraborty<sup>1</sup>

<sup>1</sup> Department of Physics and Astronomy, University of Manitoba, Winnipeg, MB R3T 2N2, Canada

<sup>2</sup> Department of Physics and Astronomy, Georgia State University, Atlanta, GA 30303, USA

Received 22 November 2007, in final form 7 February 2008

Published 13 March 2008

Online at [stacks.iop.org/JPhysCM/20/135221](http://stacks.iop.org/JPhysCM/20/135221)

## Abstract

Spin-orbit interaction in a laterally coupled double-quantum-dot system modifies both the energy spectra and the corresponding wavefunctions. These modifications introduce new features in the resonant tunneling measurements. There are new spin-orbit-induced peaks in the resonant conductance versus energy dependence. The widths and the shapes of the peaks are determined by the strength of the coupling between the states of the quantum dots. The coupling occurs through the continuous states of the leads. The width of the higher energy peak in the spin-orbit tunneling doublet is larger than the width of the lower energy peak. Spin-orbit coupling also introduces an additional interference, which results in an anti-resonant behavior of the tunneling current. We also report on our study of the interplay between the spin-orbit effects and the direct tunneling between quantum dots.

## 1. Introduction

Spin-orbit (SO) coupling in low dimensional structures [1] plays an important role in the understanding of different spin effects in semiconductor nanosystems. The SO coupling not only modifies the energy spectra of electrons, but also changes the interference and correlation properties of the electron systems through the specific structure of the electron wavefunctions in the systems with SO coupling. One of the nanosystems, in which SO coupling can result in qualitatively new effects, is a quantum dot (QD) [2]. The interest in quantum dots is related to their huge potentials for applications, ranging from novel lasers and photodetectors [3] to energy and information storing and quantum information processing [4]. The manifestation of SO coupling in the energy and the optical spectra of QDs has been studied in detail both with and without magnetic field [5, 6].

Another direction of QD research is related to coupled QDs. The coupled QDs have been proposed as building blocks of quantum computing [7]. Therefore, understanding the properties of such systems, especially in relation to their spin degrees of freedom, is very important. One very powerful and accurate tool, which is widely used to study the properties of low dimensional systems, is the measurement of electron tunneling transport through the quantum system [8]. In

such experiments either a resonant tunneling current or a current-bias voltage dependence is measured. Below we concentrate just on the resonant tunneling experiments. In these experiments the tunneling conductance at zero bias voltage is studied. As a function of a Fermi level of the leads, i.e., as a function of the gate voltage, the conductance shows a set of maxima. The condition of the maximum conductance is achieved whenever a discrete level of a system coincides with the Fermi level of the leads. Therefore, in a confined system, such as the QD, in which the energy spectra have discrete nature, it is possible to extract information about the positions of the energy levels from the resonant tunneling experiments [9]. In addition to the position, the width also characterizes the conductance maximum. The width of the conductance maximum, i.e., the width of the corresponding energy level, is determined by the coupling between the discrete levels of the system and the continuous states of the leads. This coupling has an interference nature. Since the width of the conductance maximum is determined by the interference processes, it becomes sensitive to the effects which suppress such interference. One of the types of system where such sensitivity can be observed has been discussed in [10]. In this paper a resonant tunneling through two impurities in a tunneling barrier has been studied. It has been shown that due to a coupling of the impurity states

through the continuous states of the leads, the width of the conductance resonance has strong dependence on the spatial distance between the impurities in the barrier. We explore the effect, discussed in [10], for a different structure. Namely, we consider a laterally coupled double-quantum-dot system. This system is similar to the impurity system and to study the tunneling conductance we apply the same procedure as was used in [10]. Since the width of the conductance maximum is determined by the interference processes, it is sensitive to the structure of the wavefunctions of the quantum dots. Therefore, we expect the presence of SO coupling in a double-QD system to change the shape and the width of the conductance peaks.

The problem that we study in the present paper is the resonant tunneling transport through a system of laterally coupled double QDs with SO interaction. The main question that we address in the paper is the following: what are the shapes and the widths of the conductance maxima? Since the resonant tunneling conductance is determined by the density of states of the confined system, then we just need to find the density of states of the double-QD system coupled to the leads.

The paper is organized as follows. In section 2, we present the main system of equations and the formalism that we used to study the tunneling conductance. In section 3, we present the results of calculations of the widths of the tunneling conductance peaks, which are affected by the inter-dot tunneling process. In section 4, we introduce the SO coupling and study the effect of the coupling on the widths and the shapes of the conductance peaks. In section 5 we present the concluding remarks.

## 2. Formalism

The system under consideration is shown schematically in figure 1(a). It consists of two quantum dots coupled to the right and the left leads. The Hamiltonian of the system is defined as

$$\begin{aligned}
 H = & \sum_{i=1}^2 \sum_n \varepsilon_n^i d_{i,n}^\dagger d_{i,n} - t \sum_{n,m} \left( d_{2,n}^\dagger d_{1,m} + \text{h.c.} \right) \\
 & + \sum_{k,\mu=L,R} \varepsilon_{\mu,k} c_{\mu,k}^\dagger c_{\mu,k} \\
 & + \sum_{n,k,\mu=L,R} \left( V_k^{(1)} d_{1,n}^\dagger c_{\mu,k} + V_k^{(2)} d_{2,n}^\dagger c_{\mu,k} + \text{h.c.} \right),
 \end{aligned}$$

where  $\varepsilon_n^i$  is the  $n$ th energy level of the dot  $i = 1, 2$ ,  $d_{i,n}^\dagger$  is the creation operator of an electron on the  $n$ th level of the dot  $i$ ,  $t$  is the inter-dot tunneling amplitude,  $c_{\mu,k}^\dagger$  is the creation operator of an electron with momentum  $k$  and energy  $\varepsilon_k$  in the lead  $\mu = L, R$ . Here L and R stand for the left and the right leads, respectively. The matrix elements  $V_k^{(i)}$  are the tunneling matrix elements connecting the dot  $i$  and the lead. We also assume that the inter-dot tunneling amplitude,  $t$ , has weak energy dependence.

The energy states of each QD can be found if we specify its confinement potential. For concreteness we assume that the confinement potential is parabolic for both QDs. First we study a double-QD system without SO coupling. In this case the

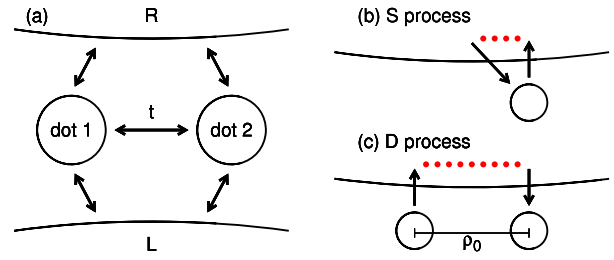


**Figure 1.** (a) Schematic illustration of a double-quantum-dot system coupled to the left (L) and right (R) leads. Here  $t$  is the amplitude of the tunneling between two dots. Schematic illustrations of the coupling of the states of QD through the continuous states of the lead for (b) the same dot (S process), and (c) different dots (D process). Here  $\rho_0$  is the inter-dot distance.

(This figure is in colour only in the electronic version)

energy levels  $\varepsilon_n^i$  of a single quantum dot can be found from the following Hamiltonian:

$$H_{\text{dot}} = \frac{\mathbf{P}^2}{2m^*} + \frac{1}{2} m^* \omega_0^2 r^2. \quad (1)$$

The eigenenergies and the eigenfunctions of the Hamiltonian (1) are the Fock–Darwin states [11], which are characterized by two quantum numbers,  $n$  and  $m$ , and have the form

$$\varepsilon_{n,m}^i = (2n + |m| + 1) \hbar \omega_0, \quad (2)$$

$$\phi_{n,m} = \frac{1}{a\sqrt{\pi}} \sqrt{\frac{n!}{(n+|m|)!}} e^{-x/2} x^{|m|/2} L_n^{|m|}(x) e^{im\theta}, \quad (3)$$

where  $L_n^{|m|}$  are the associated Laguerre polynomials [2],  $x = r^2/a^2$ , and  $a = (\hbar/m^*\omega_0)^{1/2}$  is the characteristic length of the quantum dot. The wavefunctions of the lowest six energy levels are  $\phi_{0,0}$ ,  $\phi_{0,1}$ , and  $\phi_{0,-1}$ , where the states  $\phi_{0,1}$  and  $\phi_{0,-1}$  are degenerate. To find the energy levels of the coupled QDs we need to take into account the direct tunneling between the levels of the dots. This tunneling shifts the single-dot energy levels and introduces the mixture between the states of the quantum dots.

To find the conductance  $G(E)$  through the double-dot system we have used the zero-temperature Landauer formula [12]

$$G(E) = \frac{2e^2}{h} \text{Tr} \left[ \mathbf{G}^a(E) \mathbf{\Gamma}^R \mathbf{G}^r(E) \mathbf{\Gamma}^L \right],$$

where  $\mathbf{G}^{r(a)}$  is the retarded (advanced) Green’s function of the double-dot system and  $\mathbf{\Gamma}^{L(R)}$  is the tunneling matrix, corresponding to the tunneling coupling of the dot states through the continuous states of the left (right) lead. Here  $E$  is the energy of the tunneling electron. This energy is equal to the Fermi energy of the leads. To obtain  $\mathbf{G}^r$ , we use the equation of motion approach for the retarded Green’s function. From this equation we find

$$\mathbf{G}^{r^{-1}}(E) = \begin{pmatrix} E - \varepsilon_{n,m}^1 & t \\ t & E - \varepsilon_{n,m}^2 \end{pmatrix} + \frac{i}{2} (\mathbf{\Gamma}^L + \mathbf{\Gamma}^R).$$

The coupling of the states of the dots through the continuous states of the leads is determined by two processes, which are illustrated in figures 1(b) and (c). In the first (S) process the electron tunnels from the QD into the lead states and then tunnels back into the same QD. This process determines the width of the resonant tunneling level in a single-dot system. In the double-dot system we have another (D) process, in which the electron tunnels from the state of one of the QDs into the continuous states of the lead and then tunnels into the states of another QD. As a result there is a coupling between the states of different quantum dots through the states of the lead. While the direct tunneling between the states of the QDs shifts only the positions of the resonant levels, the coupling through the continuous states modifies the width of the resonant levels of the double-dot system.

The coupling through the continuous states of the leads is described by the tunneling matrices  $\Gamma^{L(R)}$ , which have the following form:

$$\Gamma^{L(R)} = \begin{pmatrix} \Gamma_S \mathbf{M}_S & \Gamma_D \mathbf{M}_D \\ \Gamma_D \mathbf{M}_D & \Gamma_S \mathbf{M}_S \end{pmatrix}, \quad (4)$$

where  $\Gamma_S = 2\pi |V_{k_L(R)}^{(i)}|^2$ , and  $\Gamma_D = \beta \Gamma_S$ . Here, we introduce a parameter  $\beta \leq 1$ , which characterizes suppression of the inter-level coupling of different QDs compared to the coupling of the levels of the same QD. We introduce this parameter just to illustrate the interplay between different types of process, i.e. processes ‘S’ and ‘D’ shown in figure 1(b). The matrices  $\mathbf{M}_{S(D)}$  are determined by the overlap between the states of the QDs and the continuous states of the leads. For the wavefunctions (equation (3)) of the parabolic QDs the matrices  $\mathbf{M}_{S(D)}$  have the following form:

$$\begin{aligned} \mathbf{M}_S(n_1 m_1, n_2 m_2) &= \sum_k \langle n_1 m_1 | k \rangle \langle k | n_2 m_2 \rangle \delta(E - E_k) \\ &= \int d\theta_k \phi_{n_1, m_1}^*(k) \phi_{n_2, m_2}(k) \end{aligned}$$

$$\mathbf{M}_D(n_1 m_1, n_2 m_2) = \int d\theta_k \phi_{n_1, m_1}^*(k) \phi_{n_2, m_2}(k) e^{ik_0 \rho_0 \cos \theta_k},$$

where  $n_i$  and  $m_i$  are the quantum numbers of the dot  $i$  and  $k_0 = \sqrt{2m(E - E_0)}$  is the Fermi momentum of the leads. Here we assumed that the electron dispersion law in the leads is  $\varepsilon_k = E_0 + k^2/2m$  and  $E_0$  is the energy of the subband edge of the lead. Below we consider  $k_0$  as an additional parameter of the problem.

### 3. Double-QD system without SO coupling

At low temperatures and at low electron occupations of QDs, the current is determined by the tunneling through the low energy levels of the QDs. Therefore, we consider only three lowest energy levels in each quantum dot. Substituting the wavefunctions, equation (3), into the expression for matrices  $\mathbf{M}_{S(D)}$ , we obtain the matrix elements with the components corresponding to  $\{\phi_{0,0}, \phi_{0,1}, \text{ and } \phi_{0,-1}\}$  in the following form:

$$\mathbf{M}_S = \gamma \begin{pmatrix} 1 & 0 & 0 \\ 0 & k_0^2 a^2 & 0 \\ 0 & 0 & k_0^2 a^2 \end{pmatrix},$$

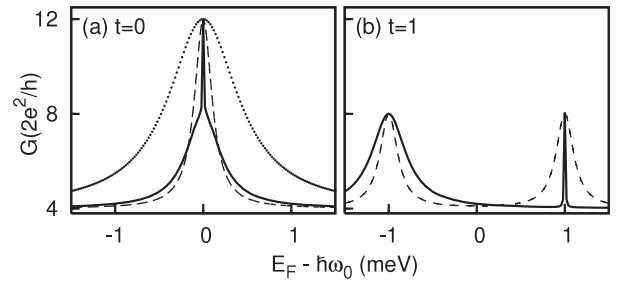


**Figure 2.** Conductance as a function of the energy of the tunneling electron is shown for a double-dot system at  $\rho_0 = 2a$  and (a)  $t = 0$  and  $\beta = 0$ ,  $k_0a = 0.002$  (dotted line),  $k_0a = 0.004$  (dashed line),  $\beta = 0.95$  and  $k_0a = 0.002$  (solid line); (b)  $t = 1$  and  $k_0a = 0.002$ ,  $\beta = 0$  (dotted line)  $\beta = 0.95$  (solid line).

$$\begin{aligned} \mathbf{M}_D &= \gamma \\ &\times \begin{pmatrix} J_0(k_0 \rho_0) & -k_0 a J_1(k_0 \rho_0) & -k_0 a J_1(k_0 \rho_0) \\ -k_0 a J_1(k_0 \rho_0) & k_0^2 a^2 J_0(k_0 \rho_0) & k_0^2 a^2 J_2(k_0 \rho_0) \\ -k_0 a J_1(k_0 \rho_0) & k_0^2 a^2 J_2(k_0 \rho_0) & k_0^2 a^2 J_0(k_0 \rho_0) \end{pmatrix}, \end{aligned} \quad (5)$$

where  $\gamma = 8\pi^2 a^2 e^{-k_0^2 a^2}$  and  $J_n$  is the Bessel function of the first kind. We can see from the above expression that on increasing the inter-dot distance,  $\rho_0$ , the coupling of the states of different QDs becomes suppressed. This suppression is not related to the suppression of the inter-dot coupling introduced by the parameter  $\beta$  in the expression for  $\Gamma_D$ . Below, we use the confinement potential strength equal to  $\hbar\omega_0 = 3$  meV and the inter-dot distance equal to  $\rho_0 = 2a$ . In general,  $\Gamma_S$  is exponentially decaying along the tunneling direction. Here, we choose  $\Gamma_S = 0.1$  meV.

First, we consider the double-dot system without direct inter-dot tunneling, i.e.,  $t = 0$ . This means that QDs are decoupled and isolated. Then the positioning of the resonant levels for a double-dot system is the same as for a single-dot system. The only effect that we should expect in such a system is the change of the widths of the resonant maxima. At small values of  $k_0a$ , the Bessel functions are approximated by  $J_0(k_0a) \simeq 1 \gg J_1(k_0a) \gg J_2(k_0a) \simeq 0$ . If the inter-dot coupling through the continuous states of the leads is suppressed, i.e.,  $\beta = 0$ , then the conductance reduces to a Lorentzian (Breit–Wigner) line shape,

$$G \simeq \left(\frac{2e^2}{h}\right) 2 \left( \frac{2\Gamma_S^2 \gamma^2}{E^2 + \Gamma_S^2 \gamma^2} + \frac{4(\Gamma_S \gamma k_0^2 a^2)^2}{(E - \hbar\omega_0)^2 + (\Gamma_S \gamma k_0^2 a^2)^2} \right), \quad (6)$$

where the factor 2 stands for the spins. The above expression has also the form of the conductance of a single dot with the conductance maximum at  $E = \hbar\omega = 3$  meV. The effective line broadening in this expression is  $\Gamma_S \gamma k_0^2 a^2$ . Therefore, on increasing the parameter  $k_0a$  the width of the resonance line is increased. This tendency is shown in figure 2(a), where we can see that the width of the peak, shown by the dashed line ( $k_0a = 0.004$ ), is four times larger than the width of the peak shown by the dotted line ( $k_0a = 0.002$ ). For the parameters of the system that we have used in our calculations, the value of  $\Gamma_S \gamma$  in the first term of equation (6) is much larger than

$E$ . Therefore, for  $E \leq 100$  meV, the contribution of the first term is around 4. This determines the background value of the tunneling conductance in figure 2. If we introduce the inter-dot coupling through the continuous states of the leads (process D), i.e., if  $\beta > 0$ , then the shape of the peak, but not its position, will be modified. For example, on a background of a broad peak we should expect the formation of a very narrow resonance line [10]. This is illustrated in figure 2(a) for  $\beta = 0.95$ .

At  $t \neq 0$ , we have a coupled double-dot system, i.e., a quantum dot molecule. The degeneracy of the energy levels ( $\phi_{0,1}$  and  $\phi_{0,-1}$ ) is lifted by the direct inter-dot tunneling. In the present problem this results in the emergence of two resonances with the same width, which is equal approximately to  $\Gamma_S \gamma k_0^2 a^2$  at  $\beta = 0$ . This behavior is shown in figure 2(b). If we introduce the coupling between the dots through the continuous states of the leads (D process), then the widths of the levels of the dots, i.e., the widths of the resonant peaks, become different. For example, the higher energy state, i.e., the unbonding state of the double-dot system, becomes narrow, while the lower energy state, i.e., the bonding state, becomes broad (see figure 2(b)). This tendency can be understood if we consider just a single level per dot. In this case, the bonding and unbonding states of the quantum dot system are symmetric and asymmetric states, respectively. The tunneling matrix becomes

$$\Gamma^{L(R)} = \begin{pmatrix} \Gamma_{11} & \Gamma_{12} \\ \Gamma_{12} & \Gamma_{11} \end{pmatrix},$$

where the quantities  $\Gamma_+$  and  $\Gamma_-$  are defined by the expression

$$\Gamma_{\pm} = \Gamma_{11} \pm \Gamma_{12}.$$

Then it can be easily shown that the conductance is the sum of two Lorentzians:

$$G \simeq \frac{2e^2}{h} \left( \frac{\Gamma_+^2}{(E-t)^2 + \Gamma_+^2} + \frac{\Gamma_-^2}{(E+t)^2 + \Gamma_-^2} \right).$$

Then the width of the bonding state is determined by  $\Gamma_+ \propto (\Gamma_{11} + \Gamma_{12})$ , while the width of the unbonding state is  $\Gamma_- \propto (\Gamma_{11} - \Gamma_{12})$ . In the present problem this means that  $\Gamma_+ \propto [1 + J_0(k_0 \rho_0)]$  and  $\Gamma_- \propto [1 - J_0(k_0 \rho_0)]$ . Therefore, for small ( $k_0 \rho_0$ ) the width of the bonding state becomes much larger than the width of the unbonding state.

#### 4. SO coupling

To include SO coupling in the double-QD system we assume that the dominant source of SO interaction is a structural inversion asymmetry [13]. Then the spin-orbit Hamiltonian takes the form [14]

$$H_{SO} = \frac{\alpha}{\hbar} [\boldsymbol{\sigma} \times \mathbf{p}]_z, \quad (7)$$

where  $z$  is the growth direction (direction of tunneling), and  $\alpha$  is the spin-orbital coupling strength. The value of  $\alpha$ , obtained from various experiments, lies in the range of 5–45 meV nm [15]. With SO coupling, determined by equation (7), the eigenfunctions of a single quantum dot can

be expressed as a linear combination of the eigenfunctions of a dot without SO coupling:

$$\Psi_{n,m} = \sum_{n',m',\sigma'} \mathbf{A}_{n',m',\sigma'}^{n,m,\sigma} \Phi_{n',m',\sigma'}, \quad (8)$$

where  $\Phi_{n,m,\sigma} = \phi_{n,m} \chi_{\sigma}$ ,  $\phi_{n,m}$  is the spatial wavefunction (see equation (3)), and  $\chi_{\sigma}$  is the spin wavefunction. We restrict the basis of a single-QD system to the six lowest energy states. These states are  $\{\Phi_{0,0,\uparrow}, \Phi_{0,0,\downarrow}, \Phi_{0,1,\uparrow}, \Phi_{0,1,\downarrow}, \Phi_{0,-1,\uparrow}, \Phi_{0,-1,\downarrow}\}$ . To find the coefficients  $\mathbf{A}_{n',m',\sigma'}^{n,m,\sigma}$  in equation (8) we need to diagonalize the matrix of the SO Hamiltonian. The elements of this matrix have the form [5]

$$\langle m \uparrow | H_{SO} | m+1 \downarrow \rangle = \begin{cases} \frac{2\alpha}{a} \sqrt{m+1} & \text{for } m \geq 0 \\ -\frac{2\alpha}{a} \sqrt{|m|} & \text{for } m < 0. \end{cases}$$

Then, after the coefficients  $\mathbf{A}_{n',m',\sigma'}^{n,m,\sigma}$  are found, the matrices  $\mathbf{M}$  in equation (4) should be replaced by  $6 \times 6$  matrices  $\mathbf{M}'_{S(D)} = \mathbf{A}^\dagger \mathbf{M}_{S(D)} \mathbf{A}$ .

From the form (7) of the SO Hamiltonian we can see that the SO interaction results in both lifting the degeneracy of the spin states of the QDs and coupling of the orbital motion with the spin degrees of freedom. These properties of the SO interaction result in new features in the resonant tunneling conductance peaks. The lifting of the degeneracy of the spin states of QDs produces double-peak structure in the  $G(E)$  dependence. The separation between the peaks and correspondingly the distance between the levels of the QD can be estimated as  $(\alpha/a)^2/\omega_0$ . It should be mentioned that in the six-state basis of the QD some states, such as  $|1 \downarrow\rangle$  and  $|-1 \uparrow\rangle$ , remain unperturbed by the SO coupling. Therefore, the energies of these states are  $\hbar\omega_0$ , i.e., they are the same as the corresponding energies in the QD without SO coupling. The energies of all other states are shifted. There is also a mixture of the states. This mixture produces the new widths of the levels of QDs even without tunneling ( $t$ ) and coupling (the D process) between the dots. Namely, one of the excited states can be written as  $|1 \uparrow\rangle + \alpha/a\omega_0 |0 \downarrow\rangle$ , where  $\alpha/a\omega_0$  is usually small. Then taking into account the expression for  $\mathbf{M}'_S$  we can find that the width of this level is proportional to  $[k_0^2 a^2 + (\alpha/a\omega_0)^2]$ . The width of the unperturbed level  $|1 \downarrow\rangle$  is proportional to  $k_0^2 a^2$ . Then the ratio of the width of the higher energy state to the width of the lower energy state is  $[1 + (\alpha/a\omega_0)^2/(k_0 a)^2]$ . Therefore, at  $(k_0 a) < \alpha/a\omega$  the lower energy resonance peak becomes narrow and the higher energy peak becomes broad. With increasing  $(k_0 a)$  the widths of two peaks become the same. This tendency is illustrated in figure 3(a), where the resonance conductance is shown for two different values of  $(k_0 a)$ . With increasing  $(k_0 a)$  the widths of the peaks are increased and finally the two peaks merge into a single peak. The behavior of a double-peak structure induced by SO splitting is completely different from the corresponding behavior in the case of the splitting due to inter-dot tunneling. As we can see in figure 2(b), for the level splitting due to the tunneling coupling, the higher energy peak is narrow while the low energy peak is broad, which is opposite to the case for the level splitting due to SO coupling.

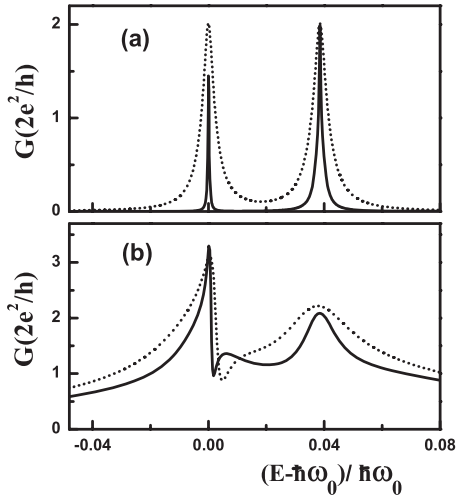


**Figure 3.** (a) Conductance as a function of energy for a tunneling electron is shown for uncoupled double quantum dots, i.e.,  $\beta = 0$  and  $t = 0$ , with spin-orbit coupling  $(\alpha/a)/\omega_0 = 0.2$  and at  $\Gamma_S/\omega_0 = 0.01$ , and  $k_0a = 0.1$  (solid line),  $k_0a = 0.4$  (dotted line). (b) Conductance is shown for a double-quantum-dot system without direct tunneling between the dots,  $t = 0$ , but with the coupling through the continuum,  $\beta = 1$ , and spin-orbit interaction,  $(\alpha/a)/\omega_0 = 0.2$ . The other parameters are  $\rho/a = 10$ ,  $\Gamma_S/\omega_0 = 0.5$ , and  $k_0a = 0.07$  (solid line),  $k_0a = 0.1$  (dotted line). Here we assume  $\gamma = 1$ .

The results in figure 3(a) are shown for uncoupled QDs, i.e., actually for a single QD. If we include the coupling between the dots, then we should expect changes not only in the widths of the two peaks but also in their shapes.

At first we assume that there is no direct tunneling between the dots, i.e., the distance between the dots is large enough. In this case we have coupling between the states of the dots only through the continuous states of the leads (the D process). Like for a single QD, the resonance conductance has a double-peak structure. If the widths of the peaks are small then the peaks have the same shape as for uncoupled dots. If we increase the widths of the resonances, i.e., if we increase  $\Gamma_S$ , then the peaks overlap and we observe the interference effects. The results of our calculations are shown in figure 3(b). Like in the single-QD behavior, the higher energy peak is broader than the lower energy one. But now we have an additional structure. Namely, at the lower energy peak there is an anti-resonant behavior and the peak acquires the features of the Fano resonance. This behavior is due to coupling between the higher energy state and the lower energy state for the different dots. This coupling results in additional interference processes in the double-dot system. At smaller values of  $\beta$ , the coupling occurs between the lower energy states of the different dots. In this case the anti-resonant behavior does not appear. What determines the anti-resonant behavior is the relative sign of  $\Gamma_S M_S$  and  $\Gamma_D M_D$ . In our case the relative sign of these two terms is controlled by the relative sign of  $M_D$  and  $M_S$  (through the Bessel functions). This sign can be positive or negative, depending on the value of  $k_0\rho_0$ .

An additional contribution to the relative sign of  $\Gamma_S M_S$  and  $\Gamma_D M_D$  (or the sign of  $\beta$ ) can arise due to a magnetic field [16]. We did not study this case in the present paper.

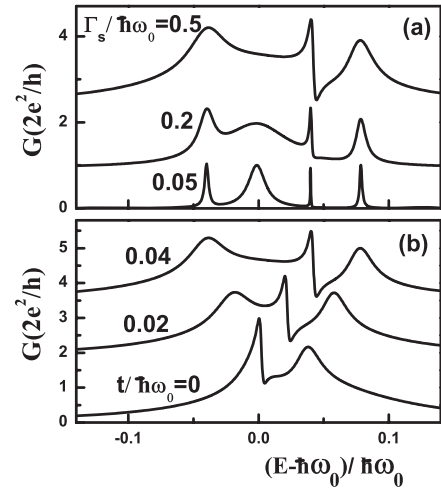


**Figure 4.** Conductance as a function of energy of the tunneling electron is shown for a coupled double-quantum-dot system with spin-orbit interaction  $(\alpha/a)/\omega_0 = 0.2$  and  $\rho/a = 10$ ,  $k_0a = 0.1$ ,  $\beta = 1$ . The other parameters are (a)  $k_0a = 0.1$ ,  $t/\hbar\omega_0 = 0.04$ , and the numbers by the lines are the values of  $\Gamma_S/\hbar\omega_0$ ; (b)  $\Gamma_S/\hbar\omega_0 = 0.5$ , and the numbers by the lines are the values of  $t/\hbar\omega_0$ . Here, we assume  $\gamma = 1$ .

If we introduce the direct tunneling between the dots, then there is an additional splitting and mixture between the states of different QDs. Generally, this should result in splitting of the SO-induced double-peak structure into the four-peak structure of the tunneling conductance. For small widths of the levels, these peaks can be, in principle, resolved. The four-peak structure is shown in figure 4(a). Here only one peak is broad and all others are narrow. We can also think about the four levels, corresponding to the peaks in the conductance, as the levels originating initially from two levels, bonding and unbonding, where the splitting between them is due to direct tunneling between QDs. Then the SO coupling introduces an additional splitting of each level. In this picture, the two higher energy levels in figure 4(a) correspond to an unbonding level with additional SO splitting, while the lower energy levels are bonding levels with SO splitting. Like for the case without SO coupling, the bonding levels are broader than the unbonding ones. If we increase the widths of the levels, i.e., increase  $\Gamma_S$ , then we can observe the interference and the anti-resonant behavior only for the unbonding levels. For the bonding levels the conductance peaks quickly merge together, resulting in a single-peak structure; see figure 4(a). The same tendency can be observed if we gradually increase the inter-dot tunneling amplitude, while keeping the strength of the SO coupling constant; see figure 4(b). At small values of the tunneling amplitude, there are two peaks, which show the interference and anti-resonant behavior. With increasing inter-dot tunneling rate these peaks become shifted to a higher energy region, but their structure remains almost the same. In addition to the higher energy peaks there is another peak at lower energies. This peak does not show any interference and has much larger width compared to the higher energy peaks.

### 5. Discussion

We have made a few assumptions during the derivation of the above results. Namely, (i) we considered only six states (with spin) per QD and then within these states we introduced the spin-orbit coupling and found the states in the QD system with SO interaction; (ii) we assumed that the inter-dot tunneling amplitude is constant and does not depend on the states of the dots; (iii) we assumed that the tunneling matrix elements,  $V_k$ , connecting the states of the dots and the leads do not depend on the states of the dots.

- (i) In the analysis of the SO coupling we considered only six levels (with spin) per dot. Strictly speaking, the SO interaction also introduces the coupling to the higher energy states. To see how strong the effect of this coupling could be on our results for the tunneling conductance, we performed the calculations for the tunneling conductance for the QD system with 30 states (with spin) per dot. We found that within the energy region of interest, the corrections to the tunneling conductance are very small. The conductance for the system with 30 states per dot is shown in figure 5(a), where the results for the system with six states (with spin) per dot are also shown. We can see that the shapes and the positions of the conductance peaks remain almost the same. Therefore the effect of the SO coupling with the higher energy states is small. Another reason that we did not consider the higher energy states in our main analysis is that the actual shape of the QD is far from the parabolic one. Then the coefficients of SO coupling between the different states of the dot are not well known. The uncertainty in these coefficients introduces corrections to the tunneling conductance, which are of the same order as or even bigger than the corrections due to the coupling to the higher energy states.

- (ii) In the above analysis we did not take into account the dependence of the inter-dot tunneling coupling on the energy of the states in the QD. The origin of such dependence is the different widths of the wavefunctions outside the trapping potential. With increasing energy of the states the width of the wavefunction is increased. Therefore the inter-dot tunneling amplitude is increased with increasing energy of the QD state [17]. With SO coupling we have a mixture of the states with different energies. Therefore we should expect a manifestation of the energy dependence of the inter-dot tunneling coupling on the tunneling conductance. We calculated the tunneling conductance taking into account the energy dependence of the inter-dot coupling and found that the tunneling conductance remains almost the same. The reason for such weak dependence of the tunneling conductance on the inter-dot coupling is the following. We consider the tunneling conductance within the energy region of the first excited state of the QD. For the first excited state the main effect of the SO coupling is the mixture of the ground state of the dot. Such mixture is relatively small: about 10%. The inter-dot tunneling coupling for the ground state is smaller than for the excited states. Then the corrections

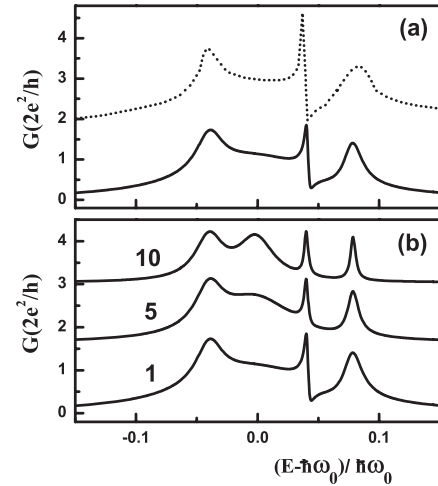


**Figure 5.** Conductance as a function of the energy of the tunneling electron is shown for a coupled double-quantum-dot system with spin-orbit interaction  $(\alpha/a)/\omega_0 = 0.2$  and  $\rho/a = 10$ ,  $k_0a = 0.1$ ,  $\beta = 1$ ,  $t/\hbar\omega_0 = 0.04$ ,  $\Gamma_S/\hbar\omega_0 = 0.5$ . In panel (a) the numbers of states (with spin) per dot are 6 (solid line) and 30 (dotted line). In panel (b) the numbers by the lines are the ratios of the tunneling matrix elements,  $V_k$ , for the excited state and the ground state of the dot.

to the inter-dot coupling of the excited states due to the admixture of the ground state is small.

- (iii) In the above analysis we assumed that the tunneling matrix elements,  $V_k$ , connecting the states of the dots and the states of the leads do not depend on the energy. This assumption is very important in our analysis. The main effect of the SO coupling is the mixture of the first excited state and the ground state of the dot. For the first excited state the admixture of the ground state is small. But the inter-dot coupling through the continuous states of the leads is much stronger for the ground state than for the excited states. This is because the inter-dot couplings are proportional to the corresponding Bessel functions (see equation (5)). Then the SO coupling strongly affects the inter-dot coupling for the excited states even for a small mixture between the states. This is opposite to the direct inter-dot tunneling coupling case (see (ii)), for which the tunneling coupling for the ground state is less than the tunneling coupling for the excited states.

At the same time the tunneling matrix element,  $V_k$ , depends on the energy of the state. The tunneling matrix element is less for the ground state than for the excited states. This will suppress the inter-dot coupling through the states of the leads for the ground state compared to the excited states. This suppression should modify the interference effects discussed in the present paper. To illustrate this tendency we introduced different tunneling matrix elements,  $V_k$ , for different states of the dot and calculated the tunneling conductance. Since we do not know exactly the profile of the tunneling barrier between the dots and the leads, we characterize the dependence of the tunneling matrix element on the state of the dot by the ratio,  $\xi$ , of  $V_k$  for the excited state and that for the ground state. The results are shown in

figure 5(b). We can clearly see suppression of interference effects with increasing  $\xi$ . At  $\xi = 10$  the conductance peaks become almost independent and decoupled.

In the above analysis we did not take into account the inter-electron interaction, assuming that this interaction is strong enough, so the presence of an additional electron moves the system to a higher energy range.

As we can see from equation (5) the interference effects discussed in the present paper are strong only for relatively small values of  $k_0a$  and  $k_0\rho$ . Therefore the wavevector,  $k_0$ , of electrons in the leads should be small. In the present approach we achieve the small value of  $k_0$  by introducing quantum wells as the leads. This means that effectively we couple the dot to the leads through the narrow quantum well. The position of the Fermi level in the quantum well can be easily varied and can take any small values.

## 6. Conclusions

We have studied the resonant tunneling conductance through the laterally coupled quantum dots with inter-dot tunneling and spin-orbit interaction. The coupling between the dots through the continuous states of the leads determines the widths of the levels of the dots and correspondingly the widths of the resonance peaks. Both inter-dot tunneling and SO coupling result in splitting of the conductance peaks. But there is a difference between these two types of splitting. Namely, for SO splitting the width of the higher energy peak in the splitting doublet is larger than the width of the lower energy peak, while for the direct tunneling splitting the width of the higher energy peak is smaller than the width of the lower energy peak. Another difference is related to the interference between the peaks due to inter-dot coupling through the continuous states of the leads. The interference pattern, which results in the anti-resonant behavior, is observed only for SO splitting of the unbonding (anti-symmetric) states of the double-dot system. In our analysis we assumed that the temperature is small, i.e., the temperature is much smaller than the inter-level spacing introduced by inter-dot tunneling and SO coupling.

## Acknowledgments

The work was supported by the Canada Research Chair Program and a Canadian Foundation for Innovation Grant.

## References

- [1] Awschalom D D, Loss D and Samarth N (ed) 2002 *Semiconductor Spintronics and Quantum Computation* (Berlin: Springer)  
Grundler D 2002 *Phys. World* **15** (4) 39  
Wolf S A *et al* 2001 *Science* **294** 1488  
Prinz G A 1995 *Phys. Today* **48** (4) 58
- Schmidt G, Gould C and Molenkamp L W 2004 *Physica E* **25** 150
- [2] Chakraborty T 1999 *Quantum Dots* (Amsterdam: Elsevier)  
Chakraborty T 1992 *Comment. Condens. Matter Phys.* **16** 35
- [3] Krishna S, Raghavan S, von Winckel G, Stintz A, Ariyawansa G, Matsik S G and Perera A G U 2003 *Appl. Phys. Lett.* **83** 2745
- [4] Eriksson M A *et al* 2004 *Quantum Inf. Process.* **3** 133  
Loss D, Burkard G and DiVincenzo D P 2000 *J. Nanopart. Res.* **2** 401
- [5] Chakraborty T and Pietiläinen P 2005 *Phys. Rev. Lett.* **95** 136603  
Chakraborty T and Pietiläinen P 2005 *Phys. Rev. B* **71** 113305
- [6] Pietiläinen P and Chakraborty T 2006 *Phys. Rev. B* **73** 155315 and references therein
- [7] Loss D and DiVincenzo D P 1998 *Phys. Rev. A* **57** 120  
Barenco A, Deutsch D, Ekert A and Jozsa R 1995 *Phys. Rev. Lett.* **74** 4083  
Landauer R 1996 *Science* **272** 1914  
Brum J A and Hawrylak P 1997 *Superlatt. Microstruct.* **22** 431
- [8] Weis J, Haug R J, von Klitzing K and Ploog K 1993 *Phys. Rev. Lett.* **71** 4019  
Schmidt T, Tewordt M, Blick R H, Haug R J, Pfannkuche D, von Klitzing K, Förster A and Lüth H 1995 *Phys. Rev. B* **51** 5570  
Narihiro M, Yusa G, Nakamura Y, Noda T and Sakaki H 1997 *Appl. Phys. Lett.* **70** 105  
Horiguchi N, Futatsugi T, Nakata Y and Yokoyama N 1997 *Appl. Phys. Lett.* **70** 2294  
Thornton A S G, Ihn T, Main P C, Eaves L and Henini M 1998 *Appl. Phys. Lett.* **73** 354  
Tarucha S, Austing D G, Tokura Y, van der Wiel W G and Kouwenhoven L P 2000 *Phys. Rev. Lett.* **84** 2485  
Ota T, Ono K, Stopa M, Hatano T, Tarucha S, Song H Z, Nakata Y, Miyazawa T, Ohshima T and Yokoyama N 2004 *Phys. Rev. Lett.* **93** 66801  
Ota T, Rontani M, Tarucha S, Nakata Y, Song H Z, Miyazawa T, Usuki T, Takatsu M and Yokoyama N 2005 *Phys. Rev. Lett.* **95** 236801  
Konemann J, Haug R J, Maude D K, Fal'ko V I and Altshuler B L 2005 *Phys. Rev. Lett.* **94** 226404  
Schmidt K H, Versen M, Kunze U, Reuter D and Wieck A D 2000 *Phys. Rev. B* **62** 15879
- [9] van der Wiel W G, De Franceschi S, Elzerman J M, Fujisawa T, Tarucha S and Kouwenhoven L P 2002 *Rev. Mod. Phys.* **75** 1
- [10] Shahbazyan T V and Raikh M E 1994 *Phys. Rev. B* **49** 17123
- [11] Fock V 1928 *Z. Phys.* **47** 446  
Darwin C G 1930 *Proc. Camb. Phil. Soc.* **27** 86
- [12] Meir Y and Wingreen N S 1992 *Phys. Rev. Lett.* **68** 2512
- [13] Zawadzki W and Pfeffer P 2004 *Semicond. Sci. Technol.* **19** R1
- [14] Bychkov Yu A and Rashba E I 1984 *Pis. Zh. Eksp. Teor. Fiz.* **39** 64  
Bychkov Yu A and Rashba E I 1984 *JETP Lett.* **39** 78 (Engl. Transl.)
- [15] Grundler D 2000 *Phys. Rev. Lett.* **84** 6074  
Nitta J, Akazaki T, Takayanagi H and Enoki T 1997 *Phys. Rev. Lett.* **78** 1335  
Matsuyama T, Hu C-M, Grundler D, Meier G and Merkt U 2002 *Phys. Rev. B* **65** 155322
- [16] Silva A, Oreg Y and Gefen Y 2002 *Phys. Rev. B* **66** 195316
- [17] Simserides C D, Hohenester U, Goldoni G and Molinari E 2000 *Phys. Rev. B* **62** 13657  
Apalkov V 2006 *J. Appl. Phys.* **100** 076101